Effects of narrow gap wave resonance on a dual-floater WEC-breakwater hybrid system

Hengming Zhang[a], Binzhen Zhou[b*], Jun Zang[c**], Christopher Vogel[d], Tianhui Fan[b], Chaohe Chen[b]

[a]*College of Shipbuilding Engineering, Harbin Engineering University, Harbin 150001, China*
[b]*School of Civil Engineering and Transportation, South China University of Technology, Guangzhou 510641, China*
[c]*Department of Architecture and Civil Engineering, University of Bath, Bath, BA2 7AY, UK*
[d]*Department of Engineering Science, University of Oxford, Oxford, OX1 3PJ, UK*

ABSTRACT

The effects of gap wave resonance on the performance of a dual-floater hybrid system consisting of an oscillating-buoy type wave energy converter (WEC) and a floating breakwater are important for the design of such a hybrid system. This paper investigates the gap wave resonance by employing a two-dimensional numerical wave flume developed using the Star-CCM+ software. The maximum wave elevation in the WEC-breakwater gap and the effects of the gap wave resonance on the performance of the dual-floater hybrid system were studied. The influence of the WEC motion and the geometrical parameters of the hybrid system on the maximum wave elevation were analyzed. The maximum gap wave elevation is essentially controlled by the vertical velocity of the free surface in the WEC-breakwater gap. The gap wave resonance was found to significantly improve the wave energy extraction performance of the hybrid system. This allowed the maximum conversion efficiency to exceed the well-known limit of 0.50 for a symmetric body in single degree-of-freedom motion. The wave resonance frequencies in the WEC-breakwater gap decreased with the increase of the gap width and the WEC draft. Due to the energy extraction of the WEC, the horizontal and vertical forces on the breakwater were reduced by up to 0.79 and 0.59, respectively.

Keywords: Wave energy converter; Floating breakwater; Wave resonance; Narrow gap; Wave attenuation; Wave energy extraction.

1. Introduction

The high construction cost and low energy extraction performance of Wave Energy Converters (WECs) reduce the economic competitiveness of wave energy, which has limited the development of commercial-scale wave power operations. Integrating WECs with other structures, such as floating offshore wind platforms [1] and floating breakwaters, is an effective solution to decrease the cost of wave energy. Mustapa et al. [2] and Zhao et al. [3] introduced the concept of combining WECs with breakwaters to provide cost reductions. Additional benefits include improved wave extraction performance and cost-sharing, space-sharing, multi-functionality, which could make wave energy economically competitive and promote the development of WECs and floating breakwaters.

A widely studied integrated WEC-breakwater system utilizes Oscillating-Buoy (OB) type WECs integrated with floating breakwaters because of the higher wave energy conversion efficiency and lower requirements on seabed conditions. These systems can be sub-divided into single-floater integrated systems and dual-floater hybrid systems for two-dimensional systems. Floater shape

* Corresponding author
E-mail address: zhoubinzhen@scut.edu.cn (B.Z. Zhou); J.Zang@bath.ac.uk (J. Zang)

significantly affects the performance of a single-floater integrated system. Madhi et al. [4] found the energy-capture efficiency of the Berkeley Wedge, an asymmetric single-floater integrated system proposed by Yeung et al. [5], reached 96.34% at the resonant frequency. Zhang et al. [6] investigated four integrated systems with different bottom shapes, revealing the energy-capture efficiency of the integrated system with an asymmetric floater was much higher than that with a symmetric floater.

Dual-floater hybrid systems consist of two floaters, one being the OB-type WEC and the other being the floating breakwater. Some studies have investigated the interaction between the WEC and the floating breakwater on the performance of the dual-floater hybrid system. Zhao & Ning [7] concluded from an experiment that the wave energy extraction performance of a novel two-pontoon system consisting of a front OB-type WEC and a rear fixed pontoon was significantly better than that of the single-pontoon system without reducing the wave attenuation performance. Further, Ning et al. analytically [8] and experimentally [9] investigated the performance of a dual-pontoon floating breakwater that also acted as a WEC, revealing that the dual pontoon-PTO system broadened the effective frequency range compared with a single pontoon-PTO system with the same pontoon volume. Then, Zhao et al. [10] studied an integrated system comprising of a WEC array and a fixed breakwater by an experiment, which demonstrated that the breakwater significantly improved the performance of the WEC array. Tay [11] numerically investigated the energy generation performance and the effectiveness in attenuating the wave forces of a multiple-raft WEC integrated with a floating breakwater, and found an average capture width of greater than 1.50 m could be achieved in a typical tropical climate. Reabroy et al. [12] used Star-CCM+ software and experiments to study the hydrodynamic and power capture performance of an asymmetric WEC integrated with a fixed breakwater, showing that the maximum power efficiency of the WEC was 0.376. This introduces some new phenomena that affect the performance of the system. Fig. 1 shows the positions of different incident waves, reflected waves, and transmitted waves around the dual-floater hybrid system. Waves transmitted through the WEC will be reflected by the floating breakwater in the rear and then superposed with the transmitted waves through the WEC [13], influencing the motion and wave energy extraction performance of the WEC. Additionally, the WEC absorbs some incident wave energy, which may affect the wave attenuation performance and forces acting on the rear breakwater.

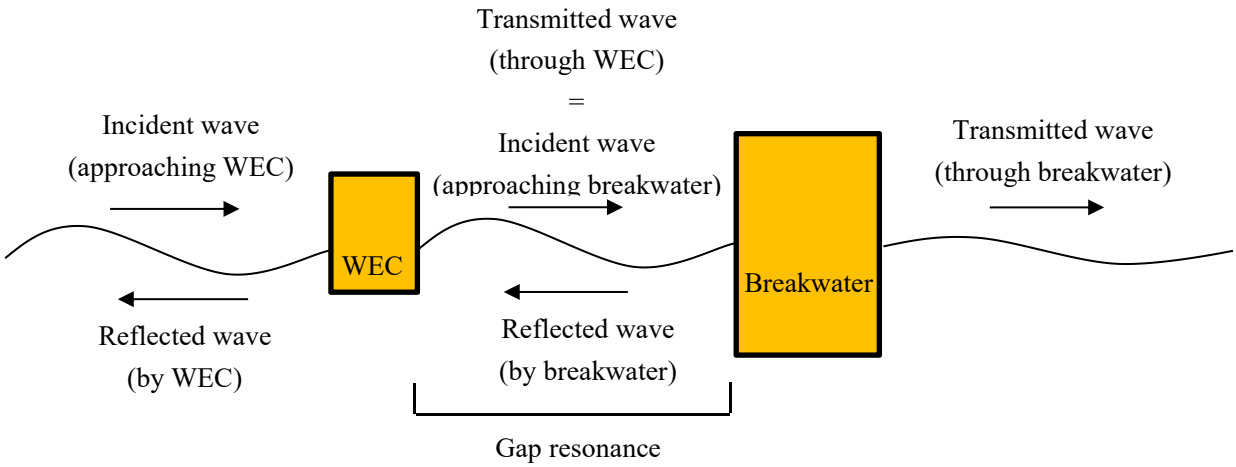

Fig. 1 Diagram indicating the different incident waves, reflected waves, and transmitted waves around the dual-floater hybrid system

The gap between the WEC and breakwater is one of the main differences between dual- and single-floater integrated systems. Under certain conditions, wave resonance may be achieved in the narrow gap, which can cause a pronounced increase in the hydrodynamic forces on the floaters and can affect the wave extraction performance of the WEC. The oscillating water column in the WEC-breakwater gap contributes to the overall energy dissipation of the hybrid system. Furthermore, the water oscillation in the WEC-breakwater gap can be taken as a radiation source for the transmitted wave from the hybrid system. Thus, it is essential to study the influence of the gap wave resonance on the performance of the hybrid system.

Previous studies on the WEC-breakwater hybrid systems have not analyzed gap resonance, and most narrow gap wave resonance investigations to date have focused on combinations of fixed and floating bodies without a PTO system. Simple numerical models based on linear potential flow theory have been widely employed to study the problem of narrow gap wave resonance. For example, Sun et al. [14] used first- and second-order wave diffraction analysis to investigate the influence of the gap wave resonance on the motion of two vessels and forces on the moorings. It is well known that the maximum wave amplitude in the gap can be overestimated by the linear potential flow theory due to the neglected effects of wave non-linearity and viscosity. Thus, some modified potential flow models considering the nonlinear free surface boundary conditions and viscous influence have been developed. To investigate the non-linear free surface effects on the gap resonance, Feng & Bai [15] established a fully nonlinear potential flow model of side-by-side barges. Their investigation demonstrated the first resonant frequency shifted but the peak value was not changed much with increasing incoming wave steepness and that the free surface nonlinearity played a minor role in suppressing the over-predicted resonance response obtained by linear models. Li & Zhang [16] employed a fully-nonlinear numerical model to investigate the influence of the barge separation, relative barge width, and draft on the wave resonance frequencies and the maximum wave elevation in the gap between two heaving barges. They concluded that the relative barge draft strongly influenced the resonance frequencies and that the gap distance can affect the type of resonance in the gap. Li [17] studied the multi-body hydrodynamic resonance and shielding effect of vessels in parallel and nonparallel side-by-side configurations, demonstrating distinct differences in the reactions to different resonant modes and that the shielding effect only suppresses the motion caused by the gap resonance.

Viscous-flow numerical models have also been employed to investigate narrow gap wave resonance. Jiang et al. [18] developed a numerical wave flume based on OpenFOAM to investigate wave resonance between two side-by-side non-identical fixed boxes and found that increasing the gap breadth and box draft can lead to a reduction of the resonant frequency. The wave forces on the boxes were studied later by Jiang et al. [19]. Numerical comparisons between the single-, two- and three-box systems were performed by Jiang et al. [20], illustrating the fluid resonance in the narrow gap can significantly affect the behavior of the box-system. Feng et al. [21] studied the viscous phenomena associated with gap resonance between two side-by-side barges using a multi-phase Navier-Stokes equations model and found that a large number of vortices were generated at the sharp corners of the barges. Besides, they also found that the incident wave steepness significantly influenced the viscous damping associated with the twin-barge system. Gao et al. [22] employed a two-dimensional (2D) numerical wave tank in OpenFOAM to investigate the free-surface elevation in the narrow gap between two side-by-side identical fixed boxes and the associated loads on the boxes. The results indicated the ratios of the second-order components of the free-surface elevation

in the gap and the moments on boxes to the corresponding first-order ones around the resonant frequency are normally larger than those at the frequencies far from the resonant frequency. Later, the wave loads during gap resonance between a fixed box and a vertical wall were also studied by Gao et al. [23], revealing the maximum horizontal wave force, the maximum vertical wave force, and the maximum moment appear to decrease with the increase of topographical slope overall.

Narrow gap resonance between two bodies has also been investigated experimentally. Zhao et al. [24] investigated the fluid response in the gap between two fixed identical barges by an experiment. Perić & Swan [25] experimentally investigated the wave excitation in the gap between a fixed and a floating body, showing that the resonance frequency in the gap related to the motion of the floating body and that resonant amplification always occurs at the resonance frequency. Ning et al. [26] studied experimentally the wave response in the gap between two barges, and the results showed that increasing the barge draft reduced the gap wave resonance frequency and that the maximum wave height in the gap was related to the draft of the lee side barge and the propagation direction of the incident wave. Zhao et al. [27] carried out an extensive set of experiments to investigate the gap resonant response under excitations of regular waves, white noise waves, and focused transient wave groups. The results revealed that transient wave group testing is a promising approach for the investigation of the gap resonance problem. The spatial and temporal structure of the gap resonance between two identical fixed boxes is investigated experimentally by Zhao et al. [28], indicating that gap resonance is a multi-modal resonant and weakly damped phenomenon.

Narrow gap wave resonance in oscillating buoy-floating breakwater hybrid system will likely demonstrate different dynamics to the non-WEC examples above due to the PTO system. Zhang et al. [29] investigated the narrow gap wave resonance of a dual-floater WEC-breakwater hybrid system using CFD software Star-CCM+, demonstrating that the wave resonance in the WEC-breakwater gap reduces the energy efficiency of the hybrid system with an asymmetric WEC but improves the energy efficiency for a symmetric WEC, and the forces on the breakwater were reduced. The maximum conversion efficiency of the hybrid system with a symmetric WEC reaches a maximum conversion efficiency η_e=0.61, which is higher than the theoretical maximum conversion efficiency of 0.50 for a symmetric heaving device. However, Zhang et al. [29] mainly focused on the hybrid system with an asymmetric WEC floater, the dynamics of narrow gap wave resonance in this case, and the effects of the geometry of the hybrid system on the breakwater forces, essential for engineering design, were not investigated.

The motivation and novelty of this paper are to investigate the reasons why the wave resonance in the WEC-breakwater gap occurs at a specific frequency and the effects of gap wave resonance on the WEC performance. The differences between wave resonance in the gap between two fixed floaters and the WEC-breakwater gap, the effects of hybrid system geometry with a symmetric WEC on the gap wave resonance frequency and the forces on the breakwater are also analyzed.

The paper is structured as follows. In Section 2, the setup of the numerical wave tank established by the CFD software Star-CCM+ is briefly introduced. In Section 3, the CFD model used in this paper is verified by comparison with other CFD results. In Section 4, the maximum wave elevation in the WEC-breakwater gap is studied, and the effects of wave resonance in the WEC-breakwater gap on the performance of the hybrid system are discussed. Then, the influence of the WEC motion and the geometry size of the hybrid system on the wave resonance frequency and the maximum wave elevation in the WEC-breakwater gap is studied. Finally, conclusions are drawn in Section 5.

2. Numerical model

A two-dimensional numerical wave flume was established using Star-CCM+ software, as shown in Fig. 2, to simulate wave interaction with a hybrid system consisting of a floating breakwater and an oscillating-buoy type WEC. In the y direction, the width of the model L_y was set to 0.01 m. The dimensions of the wave tank have been verified in a previous study [6].

As the motion of the breakwater is relatively small compared to the WEC, the breakwater was assumed to be fixed. The WEC is constrained to move only in the z direction, and the moorings of the hybrid system were not considered. The boundary conditions and mesh generation have been introduced in a previous study [29]. According to the previous investigation by Zhang et al. [6], the forcing method used at the inlet and outlet boundaries eliminates the effects of the reflected waves, and a laminar flow model was selected when the width of the floater was relatively large as in this paper.

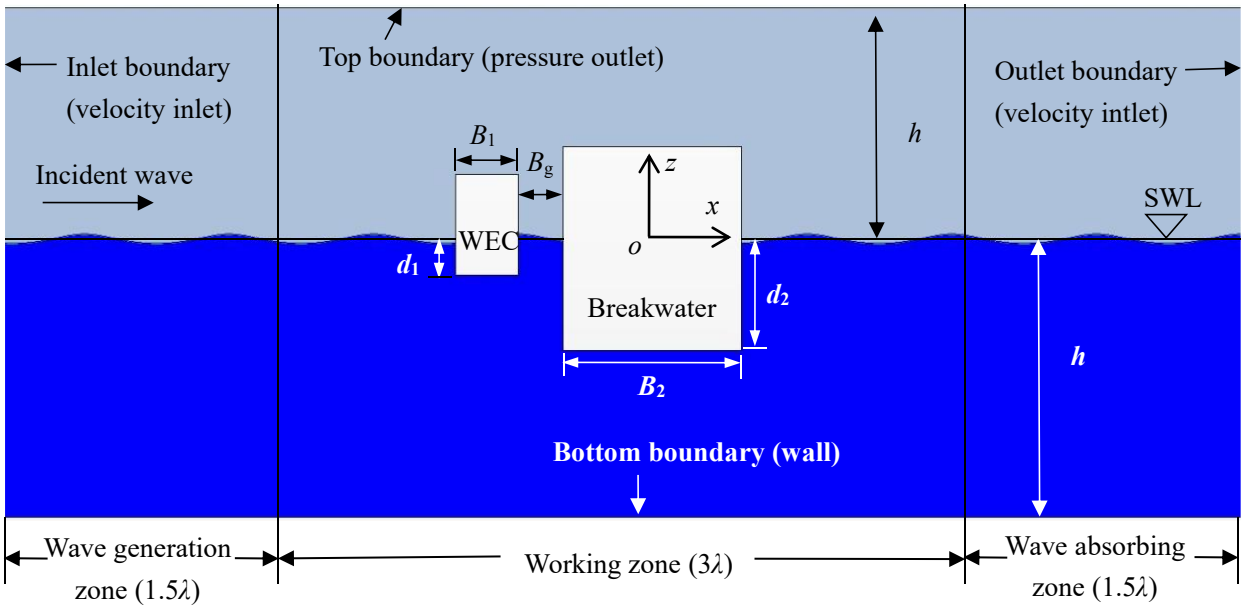

Fig. 2 A diagram of the two-dimensional numerical wave tank model (λ: wavelength).

For a single body with only a single mode of motion, the optimal damping coefficient B_{opt} under wave frequency ω can be written as

$$B_{\mathrm{opt}} = \sqrt{\frac{((m+a_{\mathrm{z}})\omega^2 - (c_{\mathrm{pto}}+c_{\mathrm{z}}))^2}{\omega^2} + b_{\mathrm{z}}^2} \tag{1}$$

where a_{z} and b_{z} are the linear added mass and radiation damping coefficients [30] [31] of the floater. $c_{\mathrm{z}}=\rho g A_{\mathrm{w}}$ is the restoring force coefficient, in which A_{w} is the wetted surface area of the floater.

The energy conversion efficiency η_{e} is expressed as

$$\eta_{\mathrm{e}} = E_{\mathrm{p}} / E_{\mathrm{w}} \tag{2}$$

where the average wave energy conversion power E_{p} and the incident wave power E_{w} are calculated as:

$$E_{\mathrm{p}} = \frac{B_{\mathrm{pto}}}{nT} \int_{t}^{t+nT} V^2 \mathrm{d}t \tag{3}$$

$$E_w = \frac{1}{16}\frac{\rho g H_i^2 \omega D_y}{k}\left(1+\frac{2kh}{\sinh 2kh}\right) \quad (4)$$

where H_i is the incident wave height, h is the water depth, V is the velocity of the floater, T is the wave period, D_y is the transverse length of the floating breakwater, and n is the number of the floater motion period.

The reflection coefficient K_r is defined as $K_r=H_r/H_i$, and the wave transmission coefficient is defined as $K_t= H_t/H_i$. The dissipation coefficient K_d is defined as

$$K_d = 1 - K_t^2 - K_r^2 - \eta_e \quad (5)$$

The ratio of floater motion amplitude H_{RAO} to the incident wave height H_i is defined as motion response ζ.

3. Verification of the numerical model

The wave-making ability of the CFD model used in this paper and the convergence of the mesh size and time step for the dual-floater model have been verified in previous studies [6] [29]. It was concluded that the dual-floater WEC-breakwater numerical model with mesh $\Delta z=H/20$, $\Delta x=2\Delta z$ and time step $\Delta t=T/1000$, which is applied in the following cases, is sufficiently accurate.

A previous study [29] compared the results of the present CFD model with the results of an experiment of a breakwater-type WEC composed of two floating pontoons with square bottoms by Zhao & Ning [7], showing the same trends between these two results. Further comparisons have been made with an OpenFOAM model consisting of two fixed non-identical boxes by Jiang et al. [18] [19], presented in Fig. 3 and Fig. 4. For the OpenFOAM model, the values of the breadths B and the drafts D of the two fixed non-identical boxes are listed in Table 1. The distance between the two boxes was B_g=0.050 m. The incident wave height H_i and water depth h were 0.012 m and 0.50 m respectively.

Table 1 The parameters of the two fixed non-identical boxes

Model	B (m)	D (m)
Front box	0.50	0.10
Rear box	0.50	0.21

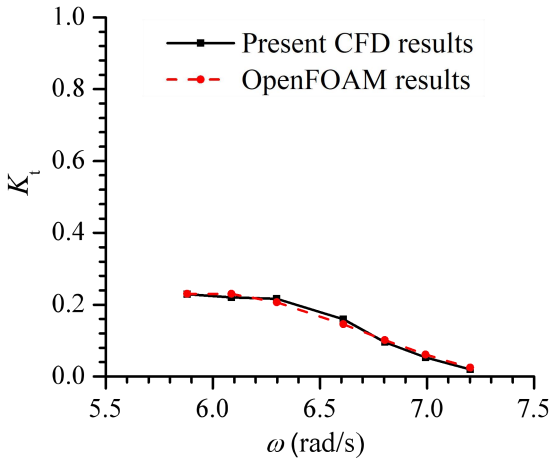

(a) Transmission coefficient

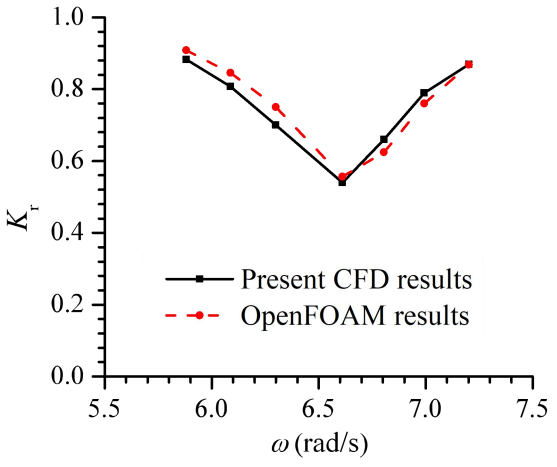

(b) Reflection coefficient

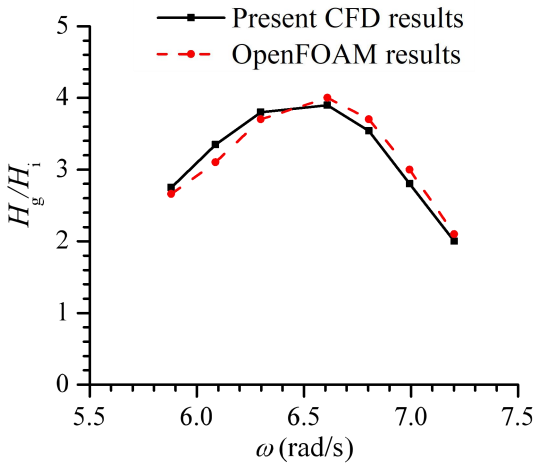

(c) Maximum wave elevation in the middle gap

Fig. 3 Comparison of transmission coefficient K_t, reflection coefficient K_r and maximum wave elevation in the middle gap H_g between the present CFD results and the OpenFOAM results of Jiang et al. (2018).

Fig. 3 compares the present CFD results with the OpenFOAM results by Jiang et al. [18], where both used the laminar flow model. It can be seen that the trends of the present CFD results agree well with those of the OpenFOAM results by Jiang et al. [18], with the differences between the two results no more than 6.60%. The present CFD results of wave forces on the second floater are also compared with those by Jiang et al. [19] in Fig. 4, which shows consistent trends. The maximum difference between these two results is less than 6.50%. Thus, the CFD model used in this paper is deemed sufficiently accurate for understanding the wave transmission, energy conversion performance, the wave forces on the breakwater, and the wave resonance in the gap of hybrid WEC-breakwater systems.

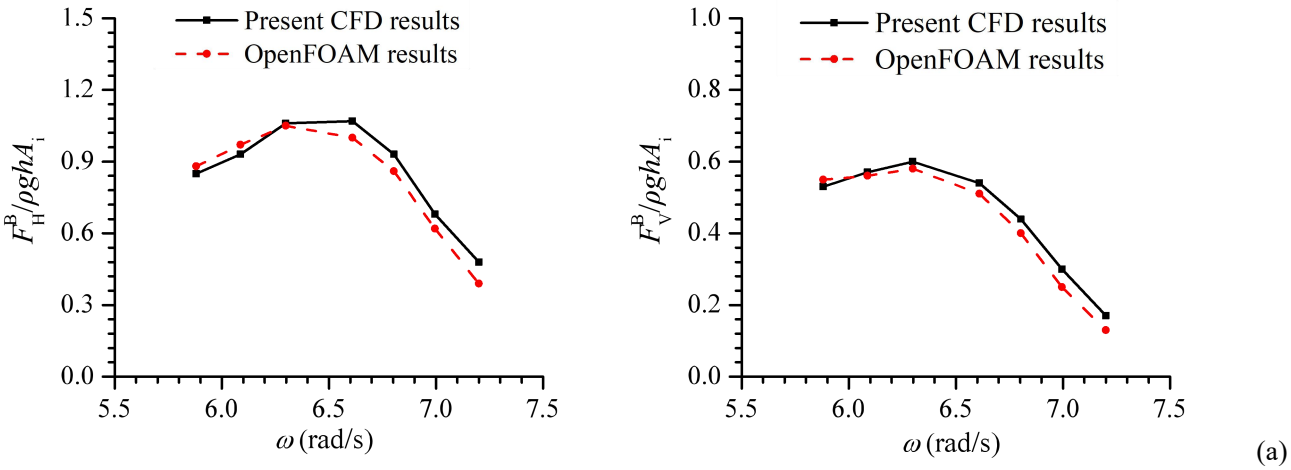

(a) Horizontal force (b) Vertical force

Fig. 4 Comparison of horizontal and vertical forces between the present CFD results and the OpenFOAM results of Jiang et al. (2018).

4. Results and discussion

4.1 Maximum wave elevation in the narrow gap

Previous investigations [29] indicated that the conversion efficiency of the hybrid WEC-

breakwater system with symmetry bottom is proportional to the maximum wave elevation in the WEC-breakwater gap. Therefore, the maximum wave elevation in the WEC-breakwater gap is investigated in this study.

For the models of the fixed structure, Jiang et al. [32] introduced that the maximum wave elevation H_g in the gap between a fixed box and a vertical wall is approximately equal to the ratio of the water volume Δ entering the box-wall gap and the gap breadth B_g, and Lu et al. [33] has reported the ratio of the average amplitude of vertical velocity V_g in the gaps between fixed rectangular structures to the maximum vertical particle velocity of incident waves V_i at the still water level is proportional to the ratio of wave height H_g in the narrow gap to the incident wave height H_i. Δ is defined as

$$\Delta = B_g \int_0^{\frac{T}{2}} \bar{v}(t) dt \tag{6}$$

where T is the wave period and $\bar{v}(t)$ is the average vertical velocity along the gap bottom.

Unlike the models of the fixed structure, the movement of the WEC floater causes the position of the WEC-breakwater gap bottom to change and thus the vertical velocity at the bottom of the gap is uncertain. To determine whether the maximum wave elevation approximation of Jiang et al. [32] and Lu et al. [33] is applicable to the WEC-breakwater hybrid system, the formulae $\Delta/B_g \approx H_g$ given by Jiang et al. [32] and $H_g/H_i \approx V_g/V_i$ given by Lu et al. [33] are investigated herein. The values of the widths B and the draft D of the WEC and the breakwater are given in Table 2. The distance between the WEC and the breakwater was B_g/h=0.083. The water depth was h=3.00 m, and the normalized incident wave height was H_i/h=0.10. The values of the optimal PTO damping B_{opt} at different frequencies ω are shown in Table 3. The vertical velocity of the free surface in the WEC-breakwater gap was used in this section to replace the uncertain vertical velocity along the WEC-breakwater gap bottom, because the gap width multiplied by the integral of instantaneous average vertical velocity at different z positions of the gap over time is always equal to the volume of water column entering the gap.

Table 2 The parameters of the WEC-breakwater hybrid system

Model	B (m)	D (m)
WEC	0.70	0.40
Breakwater	2.00	1.20

Table 3 The optimal PTO damping B_{opt} at different frequencies ω

ω (rad/s)	4.19	3.81	3.40	3.14	2.79	2.62	2.24	1.96	1.57
B_{opt} (kg/s)	7.94	8.14	9.08	10.05	11.97	13.21	16.58	19.94	26.50

Fig. 5 shows that the ratio of water volume Δ entering the WEC-breakwater gap to the gap breadth B_g and the maximum wave elevation H_g in the WEC-breakwater gap are in good agreement. From Fig. 6, it can be seen that the ratio of the vertical velocity V_g in the WEC-breakwater gap to the maximum vertical velocity of incident waves V_i correlates well with the ratio of wave height H_g in the WEC-breakwater gaps to the incident wave height H_i in general. It can be concluded from Fig. 5 and Fig. 6 that the maximum wave elevation in the WEC-breakwater gap is essentially controlled by the vertical velocity of the free surface in the WEC-breakwater gap, which is similar to the observations of Jiang et al. [32] and Lu et al. [33].

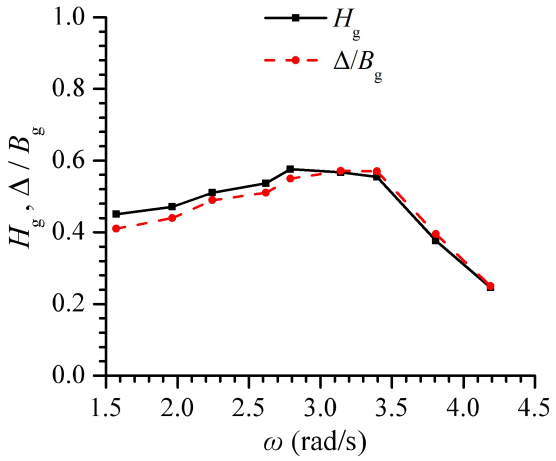

Fig. 5 Comparison of the ratio of water volume Δ entering the WEC-breakwater gap to the gap breadth B_g and the maximum wave elevation H_g in the WEC-breakwater gap.

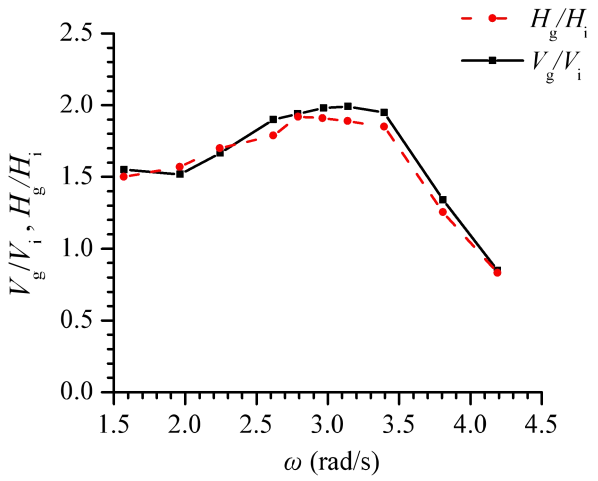

Fig. 6 Comparison of the ratio of the vertical velocity V_g in the WEC-breakwater gap to the maximum vertical velocity of incident waves V_i and the ratio of wave height H_g in the WEC-breakwater gap to the incident wave height H_i.

To further analyze the reasons why the maximum wave elevation in the WEC-breakwater gap reaches its maximum value at gap resonance frequency ω=2.79 rad/s, the time histories of wave elevations in the middle of the WEC-breakwater gap for hybrid WEC-breakwater model and corresponding positions for other models were compared, as shown in Fig. 7. It can be inferred from Fig. 7 (b) that the phase of the reflected wave by the single breakwater is similar to that of the incident wave given the slight phase difference between the curves of the single breakwater and the incident wave at resonance frequency ω=2.79 rad/s. Thus, the wave gathering function of the single breakwater at ω=2.79 rad/s is most significant, causing the amplitude of the wave elevation in front of the single breakwater to substantially increase. Similarly, the transmitted wave through the single WEC is nearly the same as that of the incident wave approaching the WEC. Therefore, the phase of the reflected wave by the breakwater of the hybrid system is also consistent with that of the incident wave through the front WEC, greatly increasing the maximum wave elevation in the WEC-breakwater gap, as shown in Fig. 7 (b). However, at non-resonance frequencies, there is a significant phase difference between the single breakwater and the incident wave, as shown in Fig. 7 (a) and (c). This demonstrates that the wave focusing performance of the breakwater is weaker at

non-resonance frequencies than at the resonance frequency, resulting in the lower maximum wave elevation in the WEC-breakwater gap.

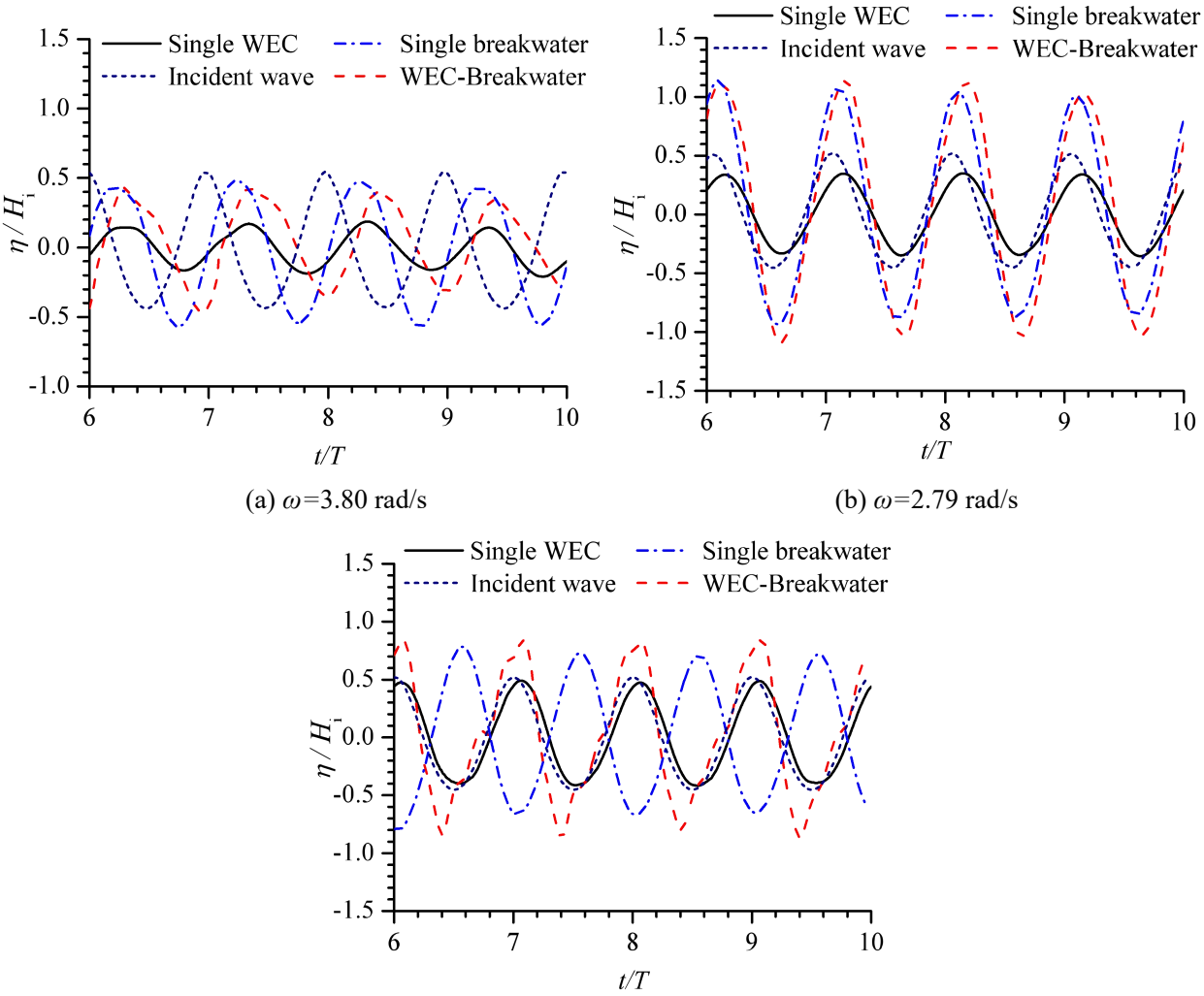

(a) ω=3.80 rad/s (b) ω=2.79 rad/s

(c) ω=1.57 rad/s

Fig. 7 Time histories of wave elevations in the middle of the WEC-breakwater gap (red-dashed line), and corresponding positions for the single WEC and single breakwater with incident wave height H_i/h=0.1.

4.2. Effect of WEC motion

Previous studies mainly focused on the wave resonance in the gap between two fixed floaters, such as Gao et al. 's investigation on two fixed floaters [22] and Jiang et al. ' s study on two non-identical boxes [18]. These studies showed that the wave resonance in the gap had a significant effect on the transmission coefficient, reflection coefficient, and energy loss coefficient. Previous investigations [29] also indicate that the wave resonance in the gap between a heaving WEC and a fixed breakwater also affects the performance of the hybrid WEC-breakwater system. In this section, the wave resonance in the gap between two fixed floaters is compared with that of the hybrid WEC-breakwater system simulated in Section 4.1, and the effects of the WEC motion on the wave resonance in the gap of the hybrid system and the breakwater forces. The system with two fixed floaters is similar to the hybrid WEC-breakwater system in Section 4.1, except that the front floater is fixed. The results of these two systems are compared in Fig. 8. All of the parameters were consistent with those of the combined breakwater-WEC system in Section 4.1.

As shown in Fig. 8 (a), the wave resonance frequencies in the gap are ω=3.14 rad/s, 2.79 rad/s for the system with two fixed floaters and the hybrid WEC-breakwater system, respectively, indicating the motion of the WEC reduces the wave resonance frequency in the gap. Compared with the system with two fixed floaters, the maximum wave elevation in the gap of the hybrid system significantly decreases, especially around the wave resonance frequency in the gap, with the maximum reduction ratio of 29.80%. This is because the WEC of the hybrid system extracts some of the incident wave energy, with the maximum conversion efficiency η_e=0.61 at wave resonance frequency ω=2.79 rad/s in the gap, as shown in Fig. 8 (b), resulting in the decrease of the vertical velocity V_g in the WEC-breakwater gap, as shown in Fig. 9

Fig. 8 (c) shows the transmission coefficient K_t is almost unchanged, as the maximum draft of the two systems is identical. A slight reduction can be observed for the hybrid WEC-breakwater system, because some of the incident wave energy is absorbed by the WEC. In the high-frequency region, the transmission coefficient K_t is almost constant. This is because the water particle velocity of short waves decays quickly increasing with water depth, and its influence on the transmission coefficient K_t reduces when the draft of the breakwater is large.

A similar trend is observed for the reflection coefficient K_r as a function of wave frequency, as shown in Fig. 8 (d). The reflection coefficient K_r of the hybrid WEC-breakwater system is always smaller than that of the system with two fixed floaters due to energy extraction by the WEC. For the fixed floater system, the minimum reflection coefficient occurs at the wave resonance frequency in the gap ω=3.14 rad/s. The reflection coefficient is also minimized at this frequency for the hybrid WEC-breakwater system, corresponding to where the combination of conversion efficiency and dissipation coefficient is large. The reflection coefficient K_r increases with wave frequency in the high-frequency region because the shorter the wavelength, the faster the water particle velocity decays with water depth.

As shown in Fig. 8 (e), the dissipation coefficient K_d of the hybrid WEC-breakwater system is smaller than that of the system with two fixed floaters when 1.96< ω <3.20 rad/s, but higher for 3.20< ω <4.19 rad/s. For the system with two fixed floaters, the maximum dissipation coefficient K_d occurs at ω=3.14 rad/s corresponding to the maximum wave elevation in the gap at the gap resonance frequency. In the hybrid WEC-breakwater system dissipation is maximized at a higher frequency of ω=3.39 rad/s with maximum K_d=0.70. The dissipation coefficient K_d in the high-frequency region is generally larger than that in the low-frequency region, because the ratio of the size of the floater to wavelength becomes larger as wave frequency increases. Viscous effects increase, leading to greater energy dissipation and thus larger K_d. However, the dissipation coefficient K_d reduces with the increasing wave frequency in the high-frequency region, because of reducing the maximum wave elevation in the gap and the increasing reflection coefficient.

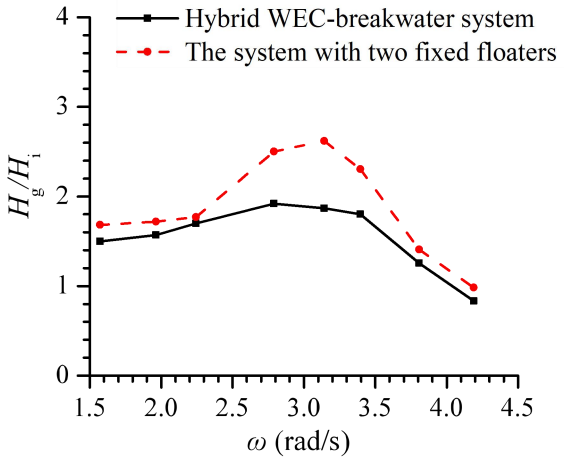

(a) Maximum wave elevation in the gap

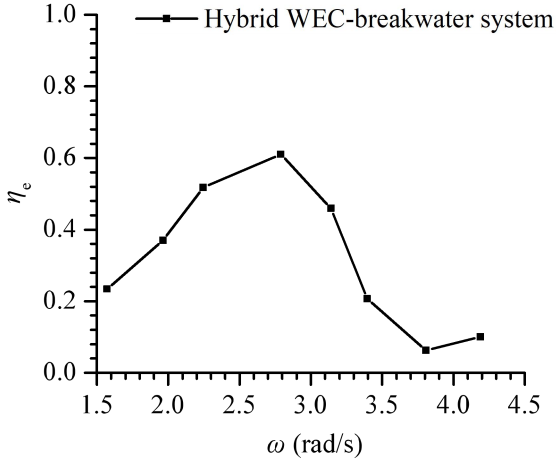

(b) Conversion efficiency

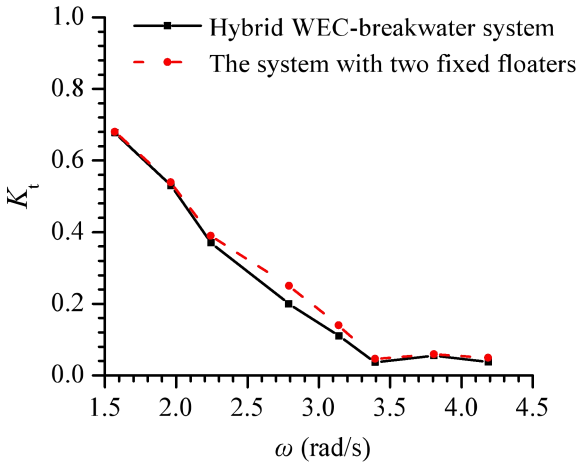

(c) Transmission coefficient

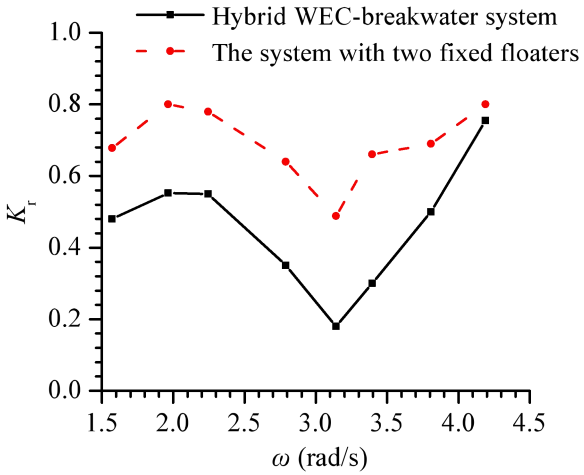

(d) Reflection coefficient

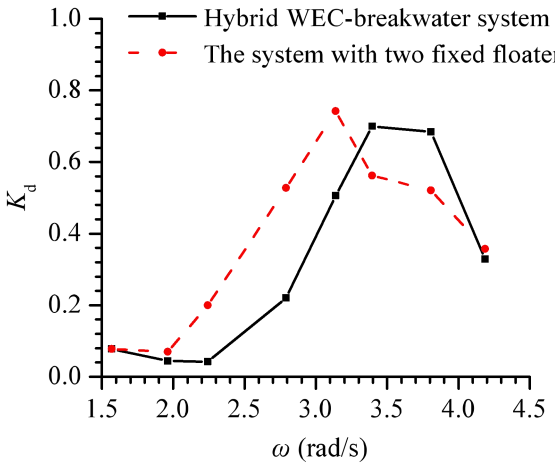

(e) Dissipation coefficient

Fig. 8 Variations of maximum gap wave elevation ratio H_g/H_i, conversion efficiency η_e, transmission coefficient K_t, reflection coefficient K_r, and dissipation coefficient K_d versus ω for the fixed floater (red) and combined WEC-breakwater hybrid (black) models under the optimal PTO.

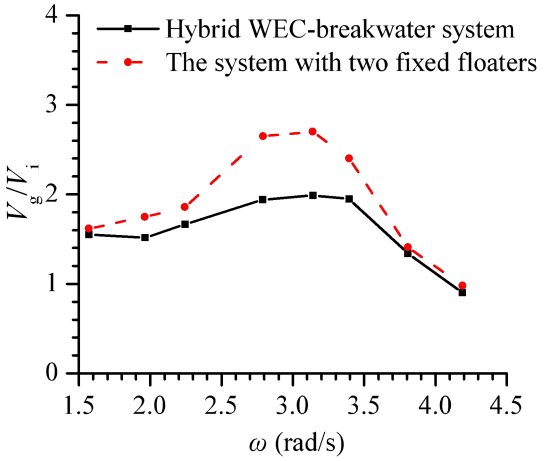

Fig. 9 Variations of gap velocity ratio V_g/V_i versus ω for the fixed floater (red) and combined WEC-breakwater hybrid (black) systems.

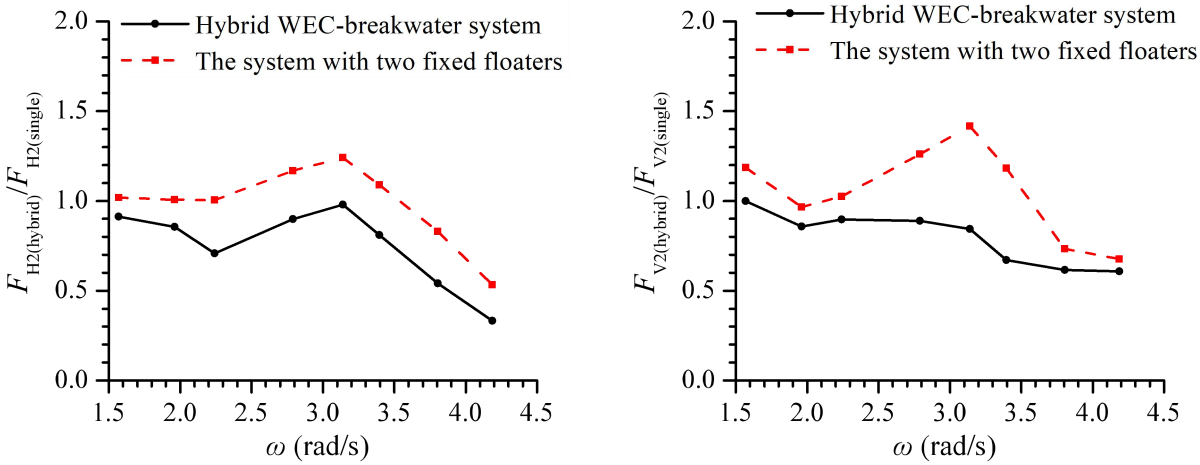

(a) Horizontal force (b) Vertical force

Fig. 10 Comparisons of horizontal and vertical forces on the breakwaters of the hybrid system with a fixed box and a heaving WEC under the optimal WEC PTO damping.

Fig. 10 compares the horizontal and vertical forces on the breakwaters of the two fixed floaters system and the hybrid WEC-breakwater system under the optimal WEC PTO damping. In both cases, similar trends are observed for the forces, albeit that the forces on the WEC-breakwater hybrid are uniformly lower than that of the fixed floater system. For ω <3.65 rad/s, the forces on the breakwater of the hybrid system with fixed floaters are bigger than that for a single breakwater, especially close to the gap wave resonance frequency, whereas the forces are lower for ω >3.65 rad/s. For the hybrid WEC-breakwater system, the forces on the breakwater are generally smaller than that of a single breakwater across all the considered wave frequencies because of the WEC absorbing part of the incident wave energy.

4.3. Effect of gap width

Three different gap widths of B_g/h=0.042, 0.083, and 0.17 were simulated to investigate the effect of the gap width between the WEC and breakwater on system performance. The other parameters were consistent with those in Section 4.1.

It can be seen from Fig. 11 (a) that the wave resonant frequency in the gap increases as the gap

width decreases because of the reduction of oscillating water volume, but that the corresponding maximum wave elevation at gap resonance frequency decreases. Similar trends were found in Jiang et al. [18] and Li & Zhang [16], for wave resonance in the gap between two fixed boxes and two heaving barges respectively. The wave resonance frequencies are ω=2.62 rad/s, 2.79 rad/s, 2.96 rad/s for B_g/h=0.042, 0.083, 0.17 respectively, which are consistent with the frequencies corresponding to the maximum energy conversion efficiency η_e in Fig. 11 (b).

Fig. 11 (b) shows the maximum energy conversion efficiency increases as the gap width decreases, with the maximum η_e=0.55, 0.61, 0.65 for B_g/h=0.042, 0.083, 0.17, respectively. When 2.24 < ω <3.70 rad/s, the energy conversion efficiency increases with decreasing gap width, as shown in Fig. 11(b). Fig. 11 (c) shows the reflection coefficient K_r significantly reduces around the wave resonance frequency in the gap, as the WEC absorbs most of the incident wave energy. The reflection coefficient K_r tends to be larger in the higher frequency region (3.14 < ω < 4.19 rad/s) for the same short wave phenomena as described in Section 4.2. Fig. 11 (d) shows the dissipation coefficient reduces with decreasing gap width when 2.24 < ω < 3.39 rad/s. The dissipation coefficient decreases as frequency increases in the high-frequency region because of the reduction in the maximum wave elevation in the gap and increase in the reflection coefficient.

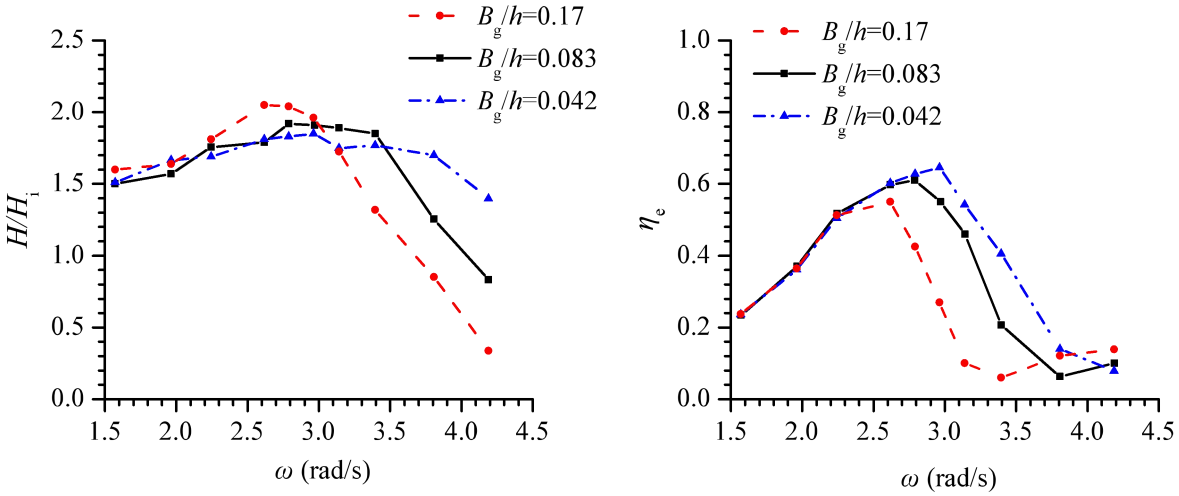

(a) Maximum wave elevation in the gap

(b) Conversion efficiency

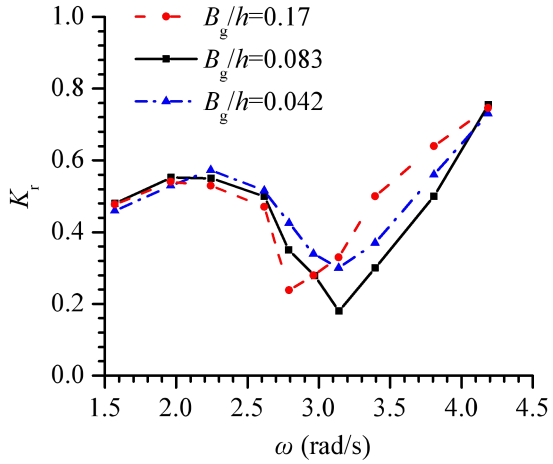

(c) Reflection coefficient

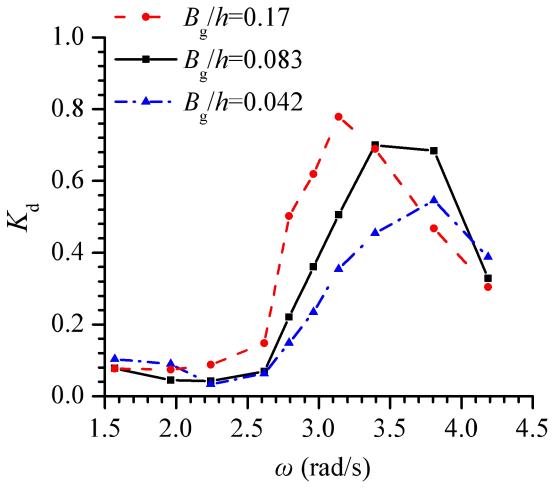

(d) Dissipation coefficient

Fig. 11 Variations of maximum gap wave elevation ratio H_g/H_i, conversion efficiency η_e, reflection coefficient K_r, and dissipation coefficient K_d versus ω for different gap widths of the hybrid system under the optimal PTO.

The vertical and horizontal forces on the breakwater of the hybrid system with different gap widths are shown in Fig. 12. From Fig. 11 (a) and Fig. 12, it can be seen that the trends of the horizontal and vertical forces on the breakwater and the maximum wave elevation in the gap with the gap width are very similar, because the forces on the breakwater are mainly related to the maximum wave elevation in front of the breakwater When 1.57< ω <3.50 rad/s, the horizontal and vertical forces both slightly reduce with decreasing gap width, but increase when 3.50< ω <4.18 rad/s because of the increase of the maximum wave elevation in the gap as gap width decreases.

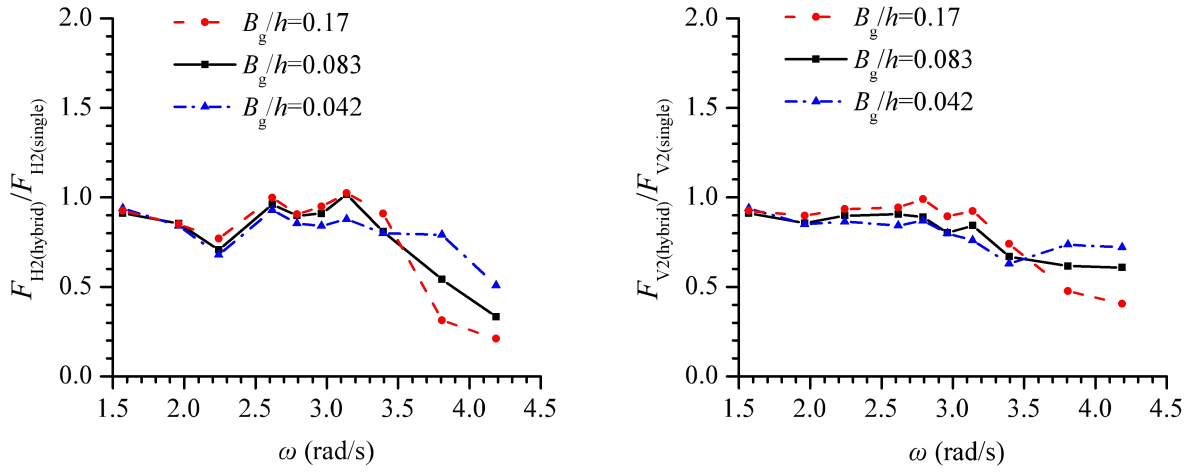

(a) Horizontal force (b) Vertical force

Fig. 12 Comparison of horizontal and vertical forces on the breakwater of the hybrid system with different gap widths between the WEC and breakwater under the optimal PTO damping.

4.4. Effect of WEC draft

To investigate the effect of the WEC draft d_1/h on the hybrid system performance, three hybrid systems with different WEC drafts d_1/h=0.17, 0.13, 0.10 were simulated. The values of the optimal PTO damping B_{opt} of the WEC with different drafts d_1 at different frequencies ω are listed in Table 4. The other parameters were consistent with those in Section 4.1.

Table 4 The optimal PTO damping B_{opt} of the WEC with different draft d_1 at different frequencies ω

ω (rad/s)	B_{opt} (rad/s)		
	d_1/h=0.17	d_1/h=0.13	d_1/h=0.10
4.18	9.84	7.94	7.32
3.81	9.13	8.14	8.09
3.40	9.18	9.08	9.50
3.14	9.73	10.05	10.69
2.96	10.38	10.95	11.67
2.79	11.24	11.97	12.75
2.62	12.35	13.21	14.04
2.24	15.60	16.58	17.39
1.96	18.98	19.94	20.71
1.57	25.66	26.50	27.18

Fig. 13 (a) shows the maximum wave elevation in the gap at gap resonance frequency increases with increasing WEC draft in the low-frequency region but decreases in the high-frequency region, consistent with the results of Jiang et al. [18]. This is because the ratio of the average amplitude of

the vertical velocity in the gap V_g to the maximum vertical velocity of the incident wave V_i reduces with decreasing WEC draft in the low-frequency region but increases with increasing WEC draft in the high-frequency region as shown in Fig. 14, and H_g/H_i is proportional to V_g/V_i as discussed in Section 4.1. The wave resonance frequency reduces from 2.96 rad/s to 2.62 rad/s as the WEC draft increases due to the corresponding increase of the water mass in the gap. The energy conversion efficiency increases as the WEC draft decreases when $2.62 < \omega < 3.65$ rad/s, as shown in Fig. 13 (b). The WEC mass is proportional to the draft, so a smaller WEC is able to heave more and thus conversion efficiency increases. The energy conversion efficiency peaks when the wave resonance in the gap occurs, with the maximum values η_e =0.57, 0.61, 0.68 for d_1/h=0.17, 0.13, 0.10 respectively. Fig. 13 (c) shows that more waves are reflected by the WEC as draft increases resulting in an increased reflection coefficient K_r, especially in the high-frequency region. Around the wave resonance frequency in the gap, the reflection coefficient K_r rapidly decreases because most wave energy is absorbed by the WEC. From Fig. 13 (d), it can be seen that the dissipation coefficient K_d suddenly decreases at the highest frequencies due to the large reflection of incoming waves and the corresponding reduction of the maximum wave elevation in the gap.

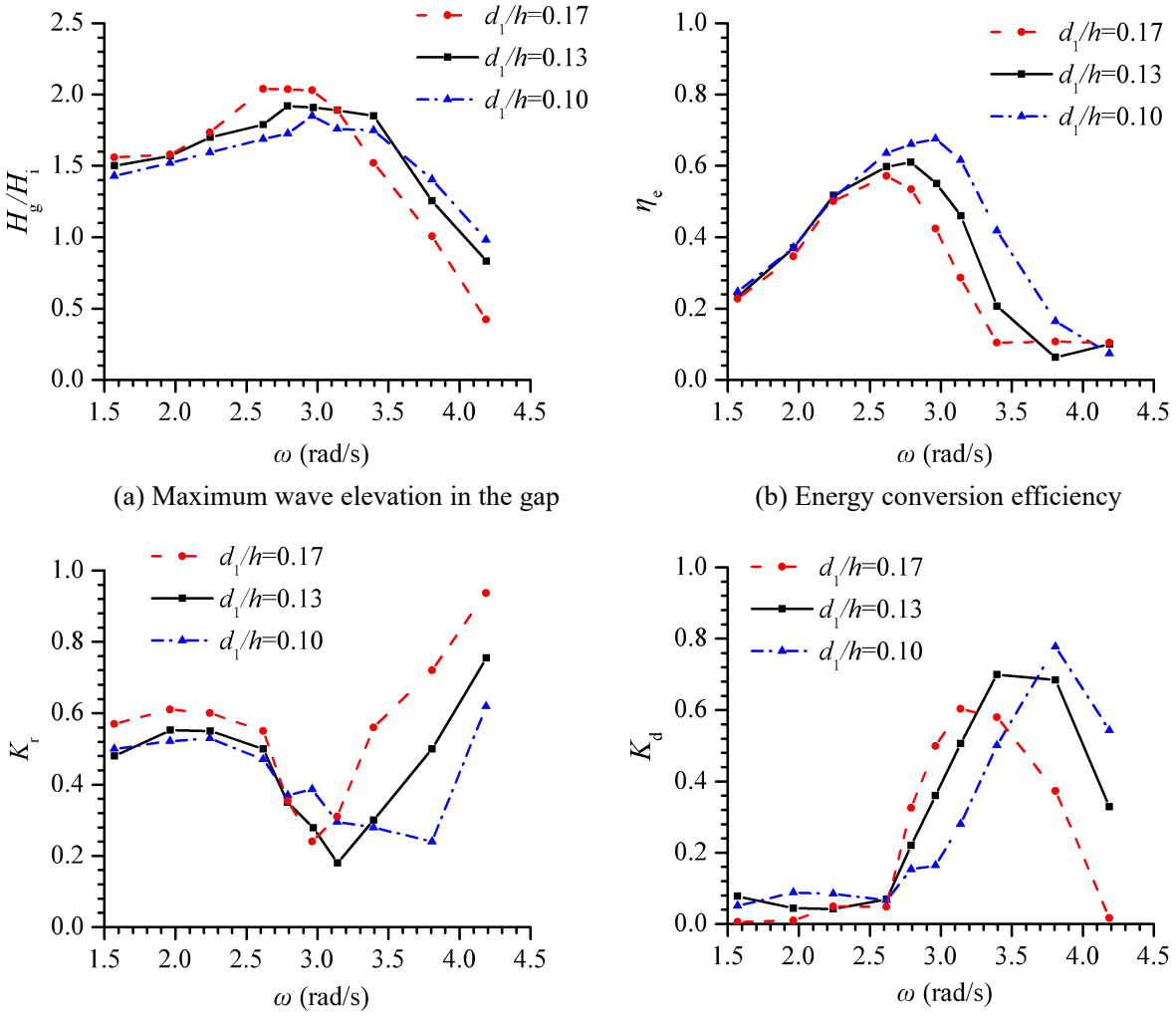

(a) Maximum wave elevation in the gap

(b) Energy conversion efficiency

(c) Reflection coefficient

(d) Dissipation coefficient

Fig. 13 Variations of maximum gap wave elevation ratio H_g/H_i, conversion efficiency η_e, reflection coefficient K_r, and dissipation coefficient K_d versus ω for hybrid systems with different WEC drafts under the optimal PTO.

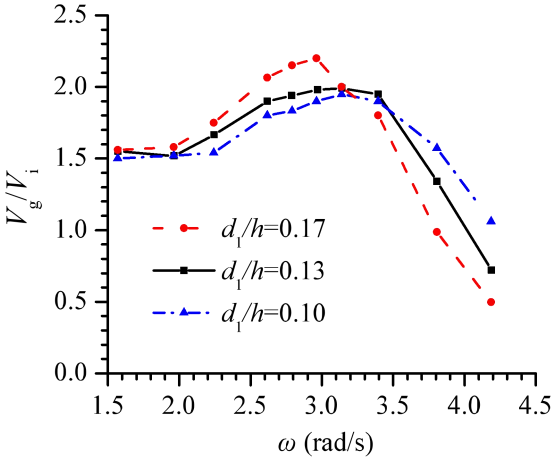

Fig. 14 Variations of gap velocity ratio V_g/V_i versus ω for different WEC drafts.

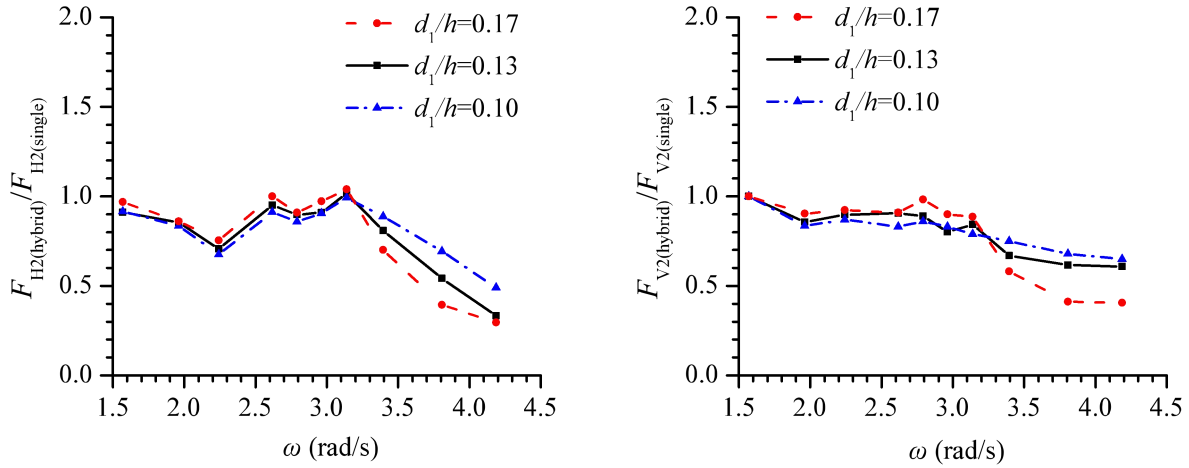

(a) Horizontal force (b) Vertical force

Fig. 15 Comparison of horizontal and vertical forces on the breakwater of the hybrid system with different WEC drafts under the optimal PTO damping.

Fig. 15 shows the vertical and horizontal forces on the breakwater of the hybrid system with different WEC drafts, indicating the forces on the breakwater slightly increase with the WEC draft for 1.57< ω <3.14 rad/s but significantly decrease at higher frequencies with WEC draft, consistent with the variation of the maximum wave elevation in the gap.

4.5. Effect of WEC width

Three different WEC widths of B_1/h=0.17, 0.23, 0.30 were considered to investigate the effect of WEC width B_1/h on the hydrodynamic performance of the hybrid system. The optimal PTO damping B_{opt} of the WEC with different widths B_1 at different frequencies ω are listed in Table 5. The other parameters were consistent with those in Section 4.1.

Table 5 The optimal PTO damping B_{opt} of the WEC with different width B_1 at different frequencies ω

ω (rad/s)	B_{opt} (rad/s)		
	B_1/h=0.17	B_1/h=0.23	B_1/h=0.30
4.18	3.81	7.94	13.86
3.81	4.22	8.14	14.09

3.40	5.43	9.08	15.01
3.14	6.50	10.05	16.29
2.96	7.39	10.95	17.07
2.79	8.34	11.97	18.23
2.62	9.47	13.21	19.66
2.24	12.34	16.58	23.68
1.96	15.13	19.94	27.83
1.57	20.44	26.50	36.13

As shown in Fig. 16 (a), the maximum wave elevation in the gap decreases with the increase of the WEC width, most significantly when ω >2.62 rad/s. This is because the increase of the WEC width leads to smaller V_g/V_i as shown in Fig. 17, and thus H_g/H_i decreases (as discussed in Section 4.1). Wave resonance in the gap occurs around ω=2.79 rad/s in all cases because the volume of the water in the gap is the same. The maximum wave elevation in the gap at gap resonance frequency H_g/H_i=2.10, 1.92, 1.91 for B_1/h=0.17, 0.23, 0.30. The conversion efficiency also peaks at the same frequency of ω=2.79 rad/s, with a maximum value η_e=0.56, 0.61, 0.68 for B_1/h=0.17, 0.23, 0.30 respectively, as shown in Fig. 16 (b). Conversion efficiency is reduced for smaller WEC widths in the low-frequency region and is nearly unchanged in the high-frequency region. Around the wave resonance frequency, the reflection coefficient K_r tends to be smaller because more wave energy is absorbed by the front WEC, with K_r=0.25, 0.18, 0.39 for B_1/h=0.17, 0.23, 0.30 at ω=3.14 rad/s, as shown in Fig. 16 (c). The significant decrease in maximum gap wave elevations and the increase of the reflection coefficient result in the reduction of dissipation coefficient K_d in the high-frequency region, as shown in Fig. 16 (d).

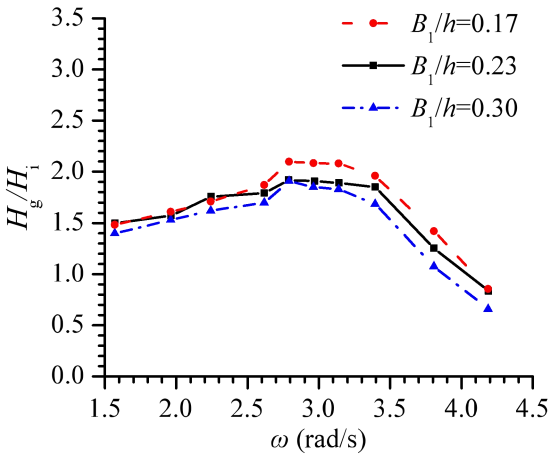

(a) Maximum wave elevation in the gap

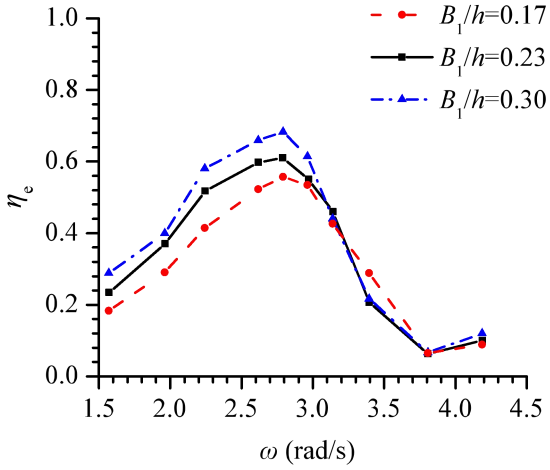

(b) Conversion efficiency

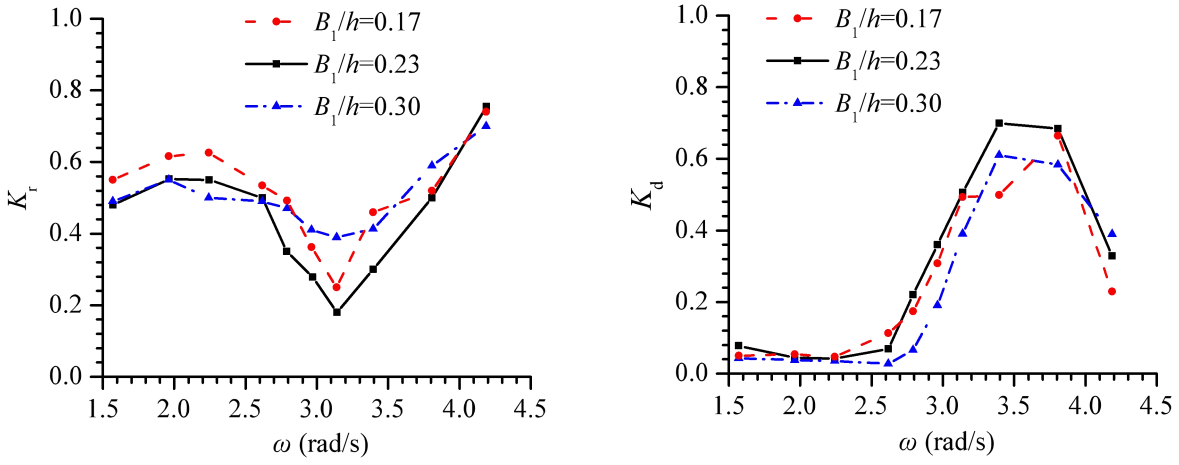

(c) Reflection coefficient (d) Dissipation coefficient

Fig. 16 Variations of the maximum gap wave elevation ratio H_g/H_i, conversion efficiency η_e, reflection coefficient K_r, and dissipation coefficient K_d versus ω for hybrid systems with different WEC widths B_1/h under the optimal PTO.

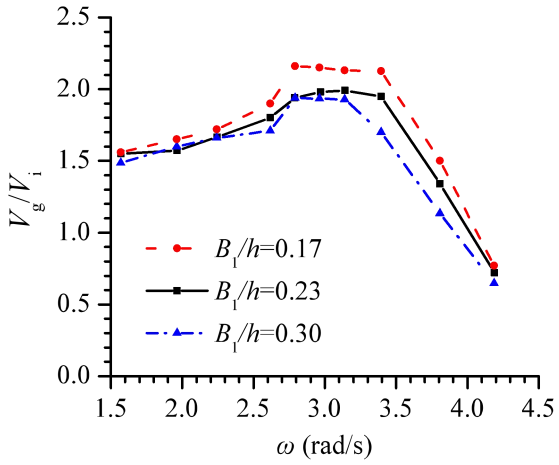

Fig. 17 Variations of gap velocity ratio V_g/V_i versus ω for hybrid systems with different WEC widths.

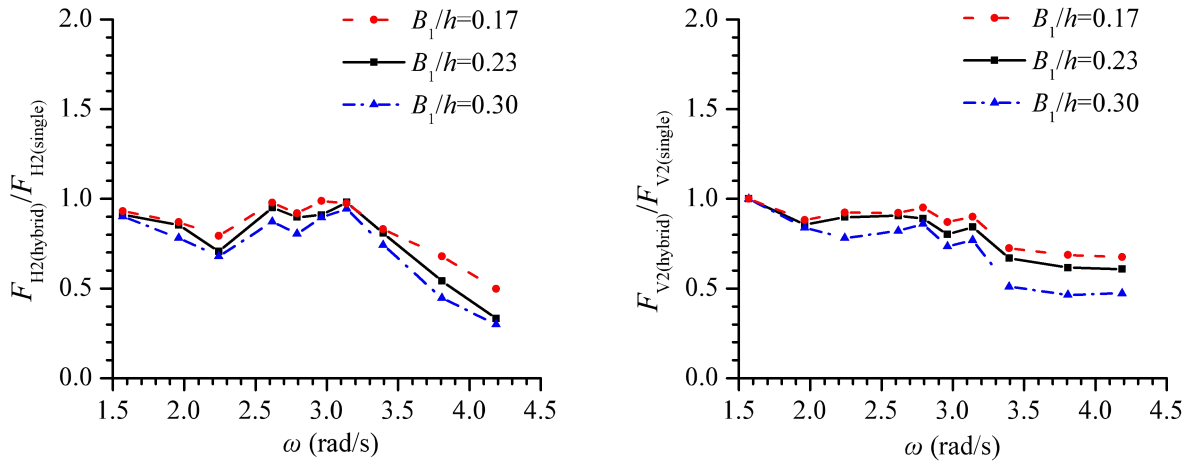

(a) Horizontal force (b) Vertical force

Fig. 18 Comparison of horizontal and vertical forces on the breakwaters of the hybrid system with different WEC widths B_1/h under the optimal PTO damping.

Fig. 18 shows that increasing the WEC width leads to the reduction of the forces on the breakwater and an increase in the energy conversion efficiency. Therefore, the WEC width of the hybrid system should be appropriately large for practical engineering applications.

5. Conclusions

In this paper, a two-dimensional numerical wave tank was developed using Star-CCM+ software to investigate the effects of the gap wave resonance on the performance of a dual-floater hybrid system consisting of an oscillating-buoy type wave energy converter and a floating breakwater and the forces on the breakwater. The influence of the WEC motion and the geometrical parameters of the hybrid system on the maximum wave elevation and resonance frequencies in the WEC-breakwater gap was also discussed. The following conclusions can be drawn from this study:

(1) The maximum wave elevation in the WEC-breakwater gap is essentially controlled by the vertical velocity of the free surface in the WEC-breakwater gap. The ratio of the average amplitude of vertical velocity in the WEC-breakwater gap to the maximum vertical particle velocity of incident waves at the still water level is proportional to the ratio of wave height in the WEC-breakwater gap to the incident wave height. The wave focusing performance of the breakwater of the hybrid WEC-breakwater system at the resonance frequency is the most significant, leading to the maximum wave elevation in the WEC-breakwater gap being the largest.

(2) The motion of the WEC leads to the decrease of the maximum wave elevation and resonance frequency in the WEC-breakwater gap, the reflection coefficient, and the forces on the breakwater of the hybrid system across the whole frequency region. In the low-frequency region $1.96< \omega <3.20$ rad/s, the dissipation coefficient of the hybrid WEC-breakwater system is smaller than that of the system with two fixed floaters, but higher when $3.20< \omega <4.19$ rad/s.

(3) The wave resonance frequency in the WEC-breakwater gap shifts to higher frequencies with the reduction of the gap width and the WEC draft, but keeps constant with the decrease of the WEC width. The maximum wave elevation in the WEC-breakwater gap at resonance frequency decreases as the gap width and the WEC draft decrease and the WEC width increases. The maximum energy conversion efficiency increases with the reduction of the gap width and the WEC draft and the increase of the WEC width. However, the transmission coefficient of the hybrid system is largely unaffected by these geometrical parameters of the hybrid system. The trends of the forces on the breakwater of the hybrid system and the maximum wave elevation in the WEC-breakwater gap with gap width, WEC draft, and WEC width are consistent.

This study provides new insights on the effects of the gap wave resonance on the performance of a dual-floater WEC-breakwater hybrid system, which will provide valuable guidance for the practical engineering design, manufacture, and optimization of the dual-floater WEC-breakwater hybrid system.

Acknowledgement

This work was supported by the National Natural Science Foundation of China (52071096, 51979111, 52071145). Student Research and Innovation Fund of the Fundamental Research Funds for the Central Universities (3072020GIP0105).

References

[1] Hu JJ, Zhou BZ, Vogle C, Liu P, et al. Optimal design and performance analysis of a hybrid system combing a floating wind platform and wave energy converters. Appl Energy 2020; 269:114998.

[2] Mustapa MA, Yaakob OB, Ahmed YM. Wave energy device and breakwater integration: A review. Renew Sustain Energy Rev 2017; 77:43-58.

[3] Zhao XL, Ning DZ, Zou QP, Qiao DS, Cai SQ. Hybrid floating breakwater-WEC system: A review. Ocean Eng 2019; 186:106126.

[4] Madhi F, Sinclair ME, Yeung RW. The Berkeley Wedge: an asymmetrical Energy-Capturing floating breakwater of high performance. Marine Syst & Ocean Tech 2014; 9(1):05-16.

[5] Yeung RW, Wehausen JV, Webster WC. Hydrodynamics of ships and ocean systems-II, lectures notes for course NAOE-241b. Tech.rep, University of California at Berkeley; 1983.

[6] Zhang HM, Zhou BZ, Vogel C, Willden R, Zang J, Zhang L. Hydrodynamic performance of a floating breakwater as an oscillating-buoy type wave energy converter. Appl Energy 2020, 257: 113996.

[7] Zhao XL, Ning DZ. Experimental investigation of breakwater-type WEC composed of both stationary and floating pontoons. Energy 2018; 155:226-233.

[8] Ning DZ, Zhao XL, Zhao M, Hann M, Kang HG. Analytical investigation of hydrodynamic performance of a dual pontoon WEC-type breakwater. Appl Ocean Res 2017; 65:102-111.

[9] Ning DZ, Zhao XL, Zhao M, Kang HG. Experimental investigation on hydrodynamic performance of a dual pontoon–power take-off type wave energy converter integrated with floating breakwaters. J Engineering for the Maritime Environment 2019; 233(4) 991–999.

[10] Zhao XL, Ning DZ, Liang DF. Experimental investigation on hydrodynamic performance of a breakwater-integrated WEC system. Ocean Eng 2019; 171: 25-32.

[11] Tay ZY. Performance and wave impact of an integrated multi-raft wave energy converter with floating breakwater for tropical climate. Ocean Eng 2020; 218:108136.

[12] Reabroy R, Zheng XB, Zhang L, Zang J, Yuan Z, Liu MY, Sun K, Tiaple Y. Hydrodynamic response and power efficiency analysis of heaving wave energy converter integrated with breakwater. Energy Convers Manage 2019; 195:1174-1186.

[13] Ren JQ, Jin P, Liu YY, Zang J. Wave attenuation and focusing by a parabolic arc pontoon breakwater. Energy 2020; 217:119405.

[14] Sun L, Eatock Taylor R, Taylor PH. Wave driven free surface motion in the gap between a tanker and an FLNG barge. Appl Ocean Res 2015; 51: 331–349.

[15] Feng X, Bai W. Wave resonances in a narrow gap between two barges using fully nonlinear numerical simulation. Appl Ocean Res 2015; 50:119-129.

[16] Li YJ, Zhang CW. Analysis of wave resonance in gap between two heaving barges. Ocean Eng 2016; 17:210-220.

[17] Li BB. Multi-body hydrodynamic resonance and shielding effect of vessels parallel and nonparallel side-by-side. Ocean Eng 2020; 218:108188.

[18] Jiang SC, Bai W, Tang GQ. Numerical simulation of wave resonance in the narrow gap between two non-identical boxes. Ocean Eng 2018; 156:38-60.

[19] Jiang SC, Bai W, Cong PW, Yan B. Numerical investigation of wave forces on two side-by-side non-identical boxes in close proximity under wave actions. Marine Struct 2019; 63:16-44.

[20] Jiang SC, Hao L, Sun TZ, Gu Q. Numerical simulation for hydrodynamic behavior of box-systems with and without narrow gaps. Ocean Eng 2020; 214:107698.

[21] Feng X, Bai W, Chen XB, Qian L, Ma ZH. Numerical investigation of viscous effects on the gap resonance between side-by-side barges. Ocean Eng 2017; 145:44-58.
[22] Gao JL, Zang J, Chen LF, Chen Q, Ding HY, Liu YY. On hydrodynamic characteristics of gap resonance between two fixed bodies in close proximity. Ocean Eng 2019; 173:28-44.
[23] Gao JL, He ZW, Zang J, Chen Q, Ding HY, Wang G. Numerical investigations of wave loads on fixed box in front of vertical wall with a narrow gap under wave actions. Ocean Eng 2020; 206:107323.
[24] Zhao W, Wolgamot HA, Taylor PH, Eatock Taylor R. Gap resonance and higher harmonics driven by focused transient wave groups. J Fluid Mech 2017; 812:905–939.
[25] Peri´c M, Swan C. An experimental study of the wave excitation in the gap between two closely spaced bodies, with implications for LNG offloading. Appl Ocean Res 2015; 51:320-330.
[26] Ning DZ, Zhu Y, Zhang CW, Zhao M. Experimental and numerical study on wave response at the gap between two barges of different draughts. Appl Ocean Res 2018; 77:14-25.
[27] Zhao WH, Pan ZY, Lin F, Li BB, Taylor PH, Efthymiou M. Estimation of gap resonance relevant to side-by-side offloading. Ocean Eng 2018; 153:1-9.
[28] Zhao WH, Taylor PH, Wolgamot HA, Molin B, Taylor RE. Group dynamics and wave resonances in a narrow gap: modes and reduced group velocity. J Fluid Mech 2019; 83, A22.
[29] Zhang HM, Zhou BZ, Vogel C, Willden R, Zang J, Geng J. Hydrodynamic performance of a dual-floater hybrid system combining a floating breakwater and an oscillating-buoy type wave energy converter. Appl Energy 2020, 259: 114212.
[30] Zhou BZ, Ning DZ, Teng B, Bai W. Numerical investigation of wave radiation by a vertical cylinder using a fully nonlinear HOBEM. Ocean Eng 2013; 70:1-13.
[31] Zhou BZ, Wu L, Xu GD. Resonance of the roll motion of a two dimensional barge induced by triple frequency wave force. Ocean Eng 2017; 134:13-23.
[32] Jiang S C, Bai W, Tang G Q. Numerical investigation of piston-modal wave resonance in the narrow gap formed by a box in front of a wall. Physics of Fluids, 2019; 052105(31).
[33] Lu L, Cheng L, Teng B, Zhao M. Numerical investigation of fluid resonance in two narrow gaps of three identical rectangular structures. Appl Ocean Res 2010; 32:177-190.